ISABE-2015-20197

Effect of Swept Stator on Fan Tone Noise of Turbofan Engine

Nobuhiko Yamasaki, Hiroki Hano, Daijiro Shiraiwa and Yuzo Inokuchi
Department of Aeronautics and Astronautics
Kyushu University
Nishi-ku, Fukuoka 819-0395 Japan

Abstract

In the present study, the fan noise due to the rotor-stator interaction is predicted and discussed on its parameter dependency. After the numerical calculation based on the three-dimensional unsteady Reynolds-averaged Navier-Stokes (URANS) equations, the acoustic modal decomposition analysis of the unsteady pressure field is conducted. The calculated sound pressure level is compared favorably with experiments, and the superiority of the present method is confirmed. The effects of the sweep angle of stator blades on the generated sound pressure level are also discussed.

Nomenclature

(r,θ,z,t)	cylindrical coordinate
$p_{\pm}(r,\theta,z,t)$	sound pressure
ℓ	axial order
m	circumferential order $m = \nu N_S + \mu N_R$
ν	order of the frequency
μ	arbitrary integer
N_R	Number of blades
N_S	Number of stator blades

Subscripts

$\pm$	aft and fore propagating waves

Introduction

In recent years, jet engines have been developed under the stringent environmental regulations. It is essential, therefore, to establish the method of numerically predicting the noise generated from jet engines with a high degree of accuracy and low cost at the development phase. Large parts of the noises generated from the jet engines are fan and jet noises. The jet noise has been reduced greatly in the current use of high bypass turbo-fan engines. The fan noise, on the other hand, is mainly caused by the rotor-stator interaction and closely related to the energy exchange between flows and blades, and the notably effective methods for reducing it have not been developed yet. The fan noise, i.e., the rotor-stator interaction noise, has two generating mechanisms. One is the noise caused by the interaction of the downstream blade rows with the wake of the upstream blade rows (wake interaction) and the other is the potential interaction caused by the relative unsteady movement of rotor blade and stator vane rows. The prediction of fan noise has been investigated using various kinds of approaches including CFD (Computational Fluid Dynamics), CAA (Computational Aeroacoustics), analytical methods and so forth [1]-[3].

As the passive noise control (PNC) for the current turbofan engines, the 3-D design of the turbomachinery is intensively used. Although this 3-D design of the turbomachinery is currently used to

actual engines in use, the mechanism of its noise suppression effects is still not fully elucidated and the estimation of the fan noise at its design stage is not routinely executed.

In Ref [4], the authors studied the effect of the lean (circumferential inclination of blades) and the rotor-stator distance, as one of the 3-D design of the turbomachinery on the fan tone noise. In the present paper, the sweep geometry (axial inclination of blades), as another 3-D design of the turbomachinery blading, is discussed numerically and its noise suppression mechanism is to be elucidated.

Fan duct modes and their decomposition

Fan noise has the tonal spectrum at the BPF (Blade Passing Frequency = Number of Rotation per seconds x Number of Rotor Blades) and its harmonics. The pressure field in the fan duct is composed analytically of the superposition of the radial and circumferential modes with discrete frequency components.

$$p_{\pm}(r,\theta,z,t) = 2\sum_{\nu=1}^{\infty}\sum_{\mu=-\infty}^{\infty}\sum_{\ell=0}^{\infty} \mathrm{Re}[FP_{\pm}(m,\ell) \times R_{m\ell}(r)\exp(i\alpha_{m\ell}z + im\theta + i\nu N_R\Omega t)] \quad (1)$$

$$\alpha_{m\ell} = \frac{1}{1-M_a^2}(\nu N_R\Omega M_a \pm \sqrt{(\nu N_R\Omega M_a)^2 - (1-M_a^2)k_{m\ell}^2}) \quad (2)$$

Here $\mathrm{Re}[\square]$ denotes the real part, $FP_{\pm}(m,\ell)$ denotes the pressure amplitude, $R_{m\ell}(r)$ and $k_{m\ell}$ denote the eigenvectors and eigenvalues for (m,ℓ) modes. The duct circumferential mode m is denoted by the number of rotor and stator blades, N_R and N_S, respectively, as

$$m = -\nu N_R + \mu N_S$$

where ν is the order of BPF and μ is an arbitrary number. Note that the rotational speed Ω is positive when the rotation is in $-\theta$ direction. For example, if $\nu = 2$ (2BPF (second BPF)), and if $\mu = -1$, then $m = 10$ ($N_R = 20$, $N_S = 30$). This sound wave has 10 wave forms in the circumferential direction and rotates spirally in the same sense as the rotor rotation at the speed of four times higher than the rotational speed of the rotor. The radial mode ℓ denotes the number of nodes in the radial direction. Each mode is denoted by the combination of the circumferential and radial orders as (n,ℓ). All modes are classified into cut-on modes which propagate in the duct without attenuation and cut-off modes which do not propagate in the duct due to attenuation. Whether the mode is cut-on or cut-off is determined by the sign of the argument of the square root in Eq.(2). If positive it is cut-on and, if not, it is cut-off. In the present method, only the cut-on modes are extracted and the acoustic prediction is executed unless otherwise noted. The inverse Fourier Bessel transformation of Eq. (1) is given by

$$FP_{\pm}(m,\ell) = \frac{N_R\Omega}{4\pi^2}\exp(i\alpha_{m\ell}z) \times \int_h^1 dr \int_0^{2\pi} d\theta \int_0^{2\pi/(N_R\Omega)} p_{\pm}(r,\theta,z,t) r R_{m\ell}(r) e^{-im\theta - i\nu N_R\Omega t} dt \quad (3)$$

Here h denotes the hub/casing ratio.

The procedure is as follows:

- Extract pressure data for one period at upstream and downstream axial location from the URANS CFD results.
- Decompose it into radial and circumferential modes to determine the modal amplitude by the inverse Fourier and Bessel analysis.
- Sound pressure is determined by decomposing into the cut-on modes.

Numerical Conditions

In the CFD analysis, the unsteady Reynolds averaged Navier-Stokes (URANS) equations are used as the fundamental equations, Roe's second-order scheme is used for the convection terms, the Spalart-Allmaras model is used as the turbulence model, and the Crank-

Nicholson method is used as the temporal second-order scheme. Figure 1 shows the baseline fan model with no-swept stator. The numerical calculations are executed for baseline geometry model, the fan model with 5-degree swept stator (Figure 2), and the fan model with 10-degree swept stator (Figure 3). The fan model has 20 rotor blade and 30 stator blades, so the 1/10 circumferential annulus with 2 rotor blades and 3 stator blade are calculated (Figure 4) . The total grid points are about 10 million in the flow field. The geometry of the baseline fan model and the experimental results were provided as the joint research program between Kyushu University and IHI Corporation[7].

Nondimensional parameters of the fan and flow condition are shown in Table 1 and Table 2.

Fig. 2 Model fan

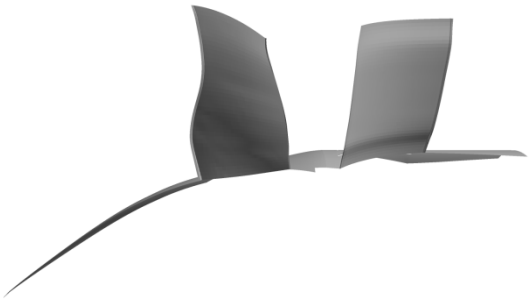

Fig. 2 Side View of 5deg. Swept Stator Model

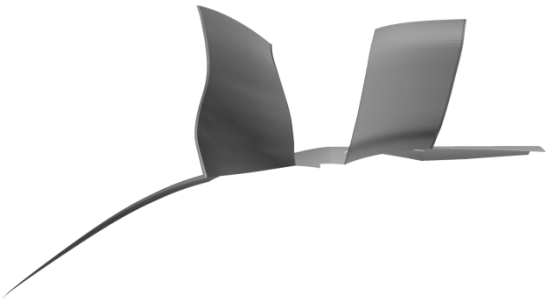

Fig. 3 Side View of 10deg. Swept Stator Model

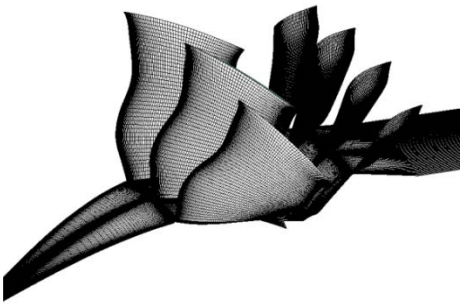

Fig. 4 Computational grid

Table 1 Nondimensional Parameters of Fan

Mean axial chord length of rotors	0.278
Mean axial chord length of stators	0.304
Boss ratio (around stators)	0.535
rotational speed 65% of operation	0.785

Table 2 Flow Condition

	Inflow	Outflow
Pressure	1 (total)	1.082 (static)
Temperature	1 (total)	-
Mach number	0.26	-

Discussion and results

At first, the results of the acoustic analysis of the baseline case are to be discussed. Figure 5 shows the instantaneous pressure variation distribution obtained by subtracting the instantaneous pressure from the time-averaged pressure over one period. The sound wave generated by the wake interaction propagates upstream through the upstream rotor passage and undergoes the potential interaction to give rise to the different wave form compared to the one propagating in the aft direction. Thus the unsteady pressure data required for the modal decomposition for the forward and aft propagating waves is extracted at the location of upstream of fan inlet and downstream of the stator blades, respectively, as is shown in Fig. 5.

Figure 6 shows the comparison of the present acoustic analysis and the experiments. For the aft propagating waves, the sound pressure level (SPL) is quite well predicted, while for the fore propagating waves, the SPL is predicted with sufficient accuracy within 5 [dB] difference from the experimental value, but the precision is not so good as the aft propagating waves. The tendency of the noise reducing order of the second-order BPF (2BPF), BPF, and the third-order-BPF (3BPF) is well reproduced in the current calculation and the validity is confirmed.

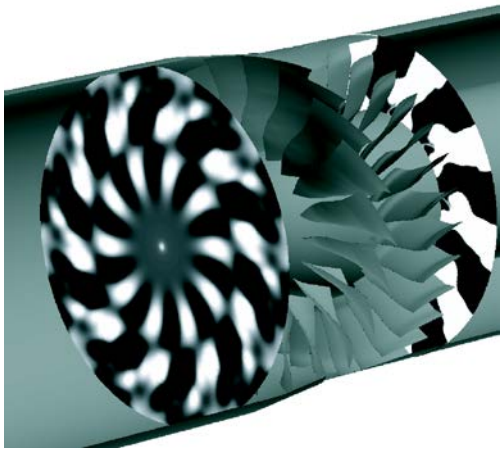

Fig. 5 Extraction position of pressure data

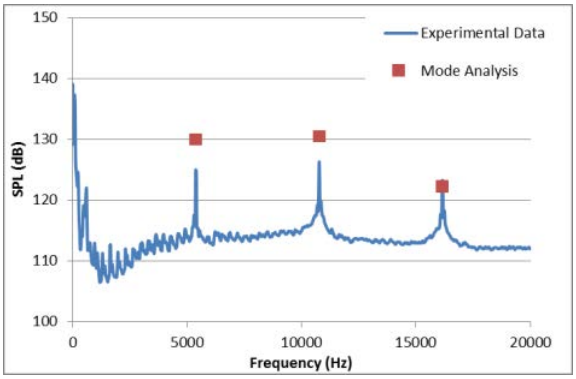

(Forward propagating)

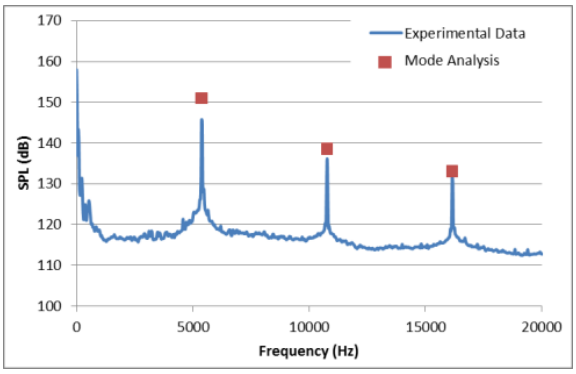

(Aft propagating)

Fig. 6 Comparison of sound pressure level (SPL)

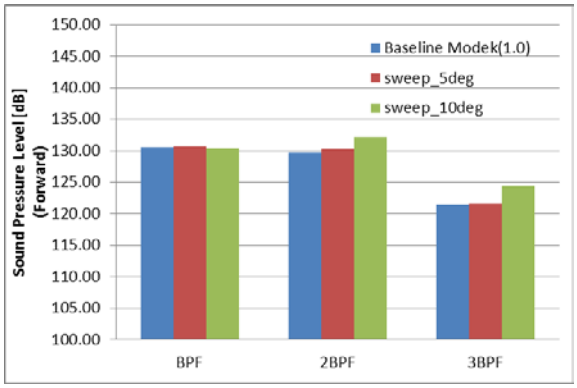

(forward propagating)

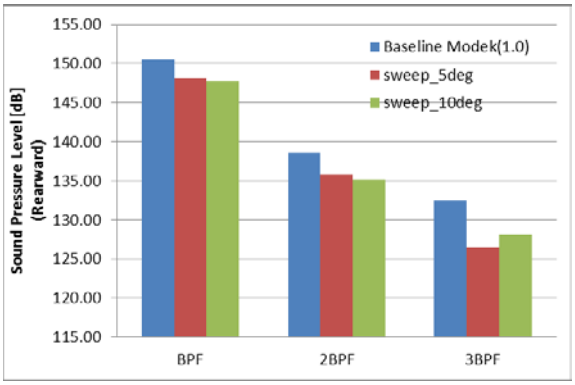

(aft propagating)

Fig. 7 Comparison of SPL

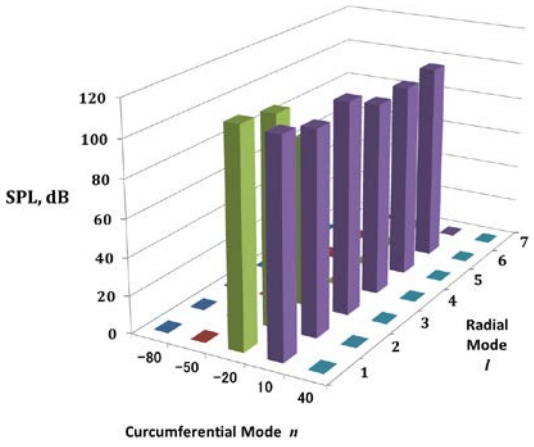

(2BPF)

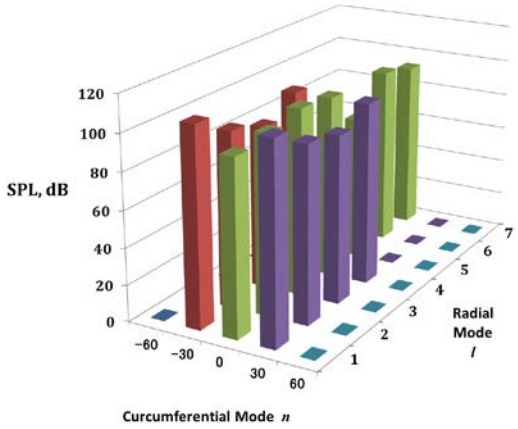

(3BPF)

Fig. 8 Cut-On Mode Distribution on Baseline Model (forward)

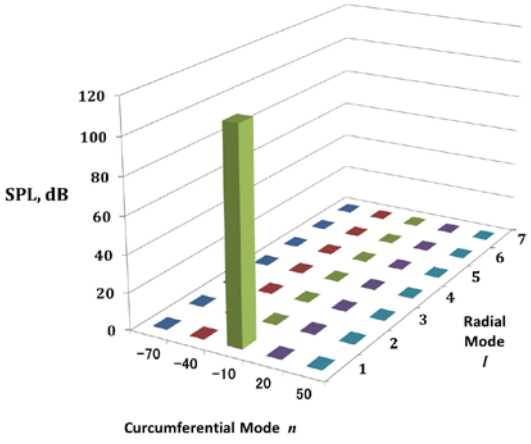

(BPF)

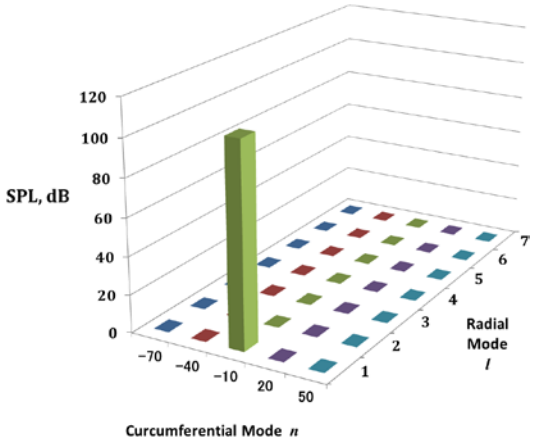

(BPF)

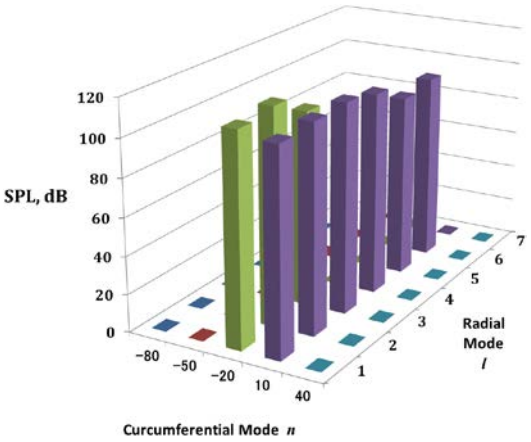

(2BPF)

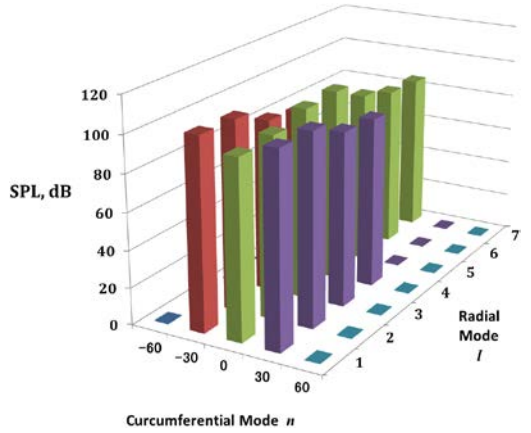

(3BPF)

Fig. 9 Cut-On Mode Distribution on 10deg. Swept Stator Model (forward)

(a) Baseline Model

(b) 10deg. Swept Stator Model

Fig.10 Instantaneous Pressure Fluctuation on Mid-Span Plane

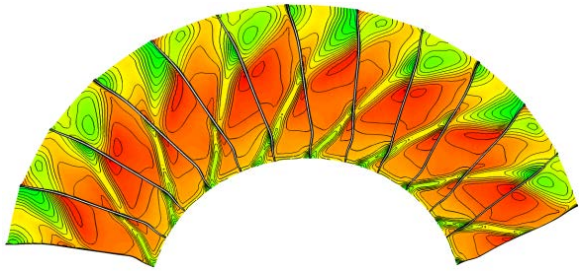

(a) Baseline Model

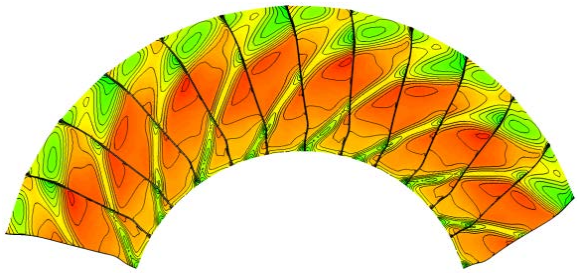

(b) 10deg. Swept Stator Model

Fig.11 Comparison of Instantaneous Total Pressure distribution

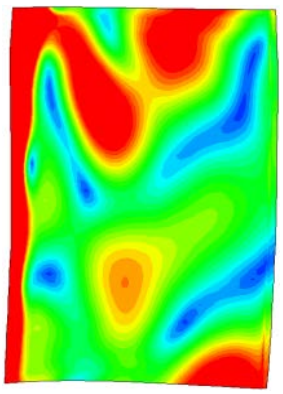

(a) Baseline Model

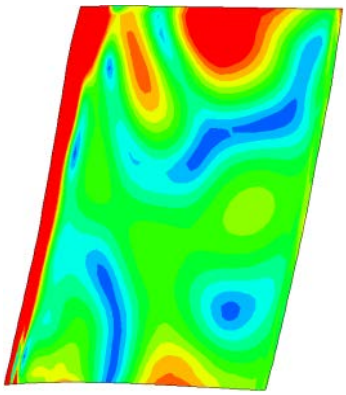

(b) 10deg. Swept Stator Model

Fig.12 Comparison of Surface Contours of the Unsteady Pressure Difference

Figure 7 shows the comparison of the numerical results of the SPL for fore and aft propagating waves. For the fore propagating waves, the swept blades in the axial direction increases the SPL by 2 [dB] in the 2BPF and 3BPF components, and its reason is not clear up to now and still under investigation. For the aft propagating waves, as much as 6 [dB] reduction is observed where the SPL is large, which can be physically explained by the interacting angle between the rotor blade wakes and the stator blades.

Figures 8 and 9 show the mode amplitude for the forward propagation wave at BPF, 2BPF and 3BPF on the baseline model and the model with 10-degree swept stator blades. The results of the modal decomposition reveal quantitatively the relative intensity of each mode. One can see that the SPL on the model with 10-degree swept stator blades is smaller, especially at first radial mode, than that on the baseline model.

Figure 10 shows the instantaneous pressure fluctuations on the mid-span plane for the baseline model and the model with 10-degree swept stator blades. The wave front are propagating spirally in the opposite direction to the stator blades. There is the wave whose form is different from that of the wave propagating from the stator blades to the rotor blades. This wave is generated by the interference between the wave propagating from the stator blades and the rotor blades. One can see the wave through the rotor blades by comparing the wave surfaces forward and aft the rotor blades.

Figure 11 shows the total pressure distribution at the axial location of the leading edge of the stator blades for the baseline model and the model with the 10-degree swept stator blades. In reference to the stator blade installation angle, the rotor blade wakes is more inclined to the hub direction at the larger radius in the model with the 10-degree swept stator than those in the non-swept baseline model. This inclination of the stator blades and the rotor-blade wakes in the direction of less parallel direction alleviated the fluctuating interference.

Figure 12 shows the unsteady pressure difference distribution on the stator blade due to the rotor-stator interaction. Since the interaction is smaller for the model with the 10-degree swept stator blades, the large unsteady pressure difference near the casing is reduced by the sweep of the stator blades and it leads to the reduction of the fan tone noise.

Conclusion

In the present paper, the acoustic mode decomposition method which predicts the fan tone noise with high precision due to the rotor-stator interaction from the numerical results of the URANS calculation is applied successfully to compare the experimental results and to applied to the acoustic mode analysis and the noise evaluation of the fan model with various sweep angles of the stator. Main conclusions are itemized as follows:

1. The mode decomposition method is successful applied to obtain the higher precision prediction of the fan tone noise.
2. By using the present method of the acoustic field analysis, the quantitative evaluation of the fore and aft propagating sound waves is facilitated. Especially, high precision prediction is obtained for all multiple BPF frequency components of the aft propagating sound waves.
3. The effect of the additional dissipation in the velocity deficit of the rotor blade due to the increased rotor-stator distance in the swept stator blade is not conspicuous, and the increased suppression of the fan tone noise is due to the more inclined interference of the rotor blade wake and the stator blades.

Acknowledgement

This research work is partly supported by JSPS KAKENHI Grant Number 23560955 and 26420813.

References

[1] Biedron, R.T., Rumsey, C.L., Podboy, G.G., and Dunn, M.H., “Predicting the Rotor-Stator Inter-action Acoustics of a Ducted Fan Engine,” 39th AIAA Aerospace Sciences Meeting & Exhibit, AIAA Paper 2001-0664, Jan. 2001.

[2] Polacsec, C., Burguburu, S., Redonnet, S., and Terracol, M., “Numerical Simulations of Fan Interaction Noise Using a Hybrid Approach,” AIAA Journal, Vol. 44, No. 6, pp. 1188-1196, Jun. 2006.

[3] Yamasaki, N., and Shiraiwa, D., “Fan Noise Prediction Using Unsteady CFD Analysis and Modal Decomposition”, Proceedings of 21st International Symposium on Air Breathing Engines (ISABE) Busan Korea, 2013

[4] Tyler, J.M., and Sofrin,T.G., “Axial Flow Compressor Noise Studies,” Transactions of the Society of Automotive Engineers, 70, 309-332, 1962

[5] Tsuchiya, N., Nakamura, Y., Yamagata, A., and Kodama, H., “Fan Noise Prediction Using Unsteady CFD Analysis,” 8th AIAA/CEAS Aeroacoustics Conference, AIAA Paper 2002-2491, 2002.

[6] Tsuchiya, N., Nakamura, Y., Yamagata, A., and Kodama, H., “Investigation of Acoustic Modes Generated by Rotor-Stator Interaction,” 9th AIAA/CEAS Aeroacoustics Conference, AIAA Paper 2003-3136, 2003.

[7] Tanigawa, K., Yamasaki, N., and Ooishi, T., “Improved Hybrid Prediction of Fan Noise,” 11th AIAA/CEAS Aeroacoustics Conference, AIAA Paper 2009-3341, 2009.

[8] Oba, Y., Ideta, T., and Ooishi, T., “Low Noise Research and Development in Japanese Environmentally Compatible Engine for Small Aircraft Project,” Proceedings of the International Gas Turbine Congress 2007 Tokyo, IGTC2007-TS-024, 2007.

[9] Yamane, T., Yamamoto, K., Enomoto, S., Yamazaki, H., Takaki, R., and Iwamiya, T., “Development of a Common CFD Platform -UPACS-,” Proceedings of the Parallel Computational Fluid Dynamics 2000 Conference, pp. 257-264, Elsevier Science B.V., 2000